AIAA SciTech Forum
8-12 January 2024, Orlando, FL
AIAA SCITECH 2024 Forum

10.2514/6.2024-1166

Optimizing UAV Network Efficiency: Integrative Strategies for Simultaneous Energy Management and Obstacle-Aware Routing

Salar Basiri*†
University of Illinois at Urbana-Champaign, Urbana, IL, 61801

Dhananjay Tiwari‡
University of Illinois at Urbana-Champaign, Urbana, IL, 61801

Christos Papachristos§
University of Nevada, Reno, Reno, NV, 89557

Srinivasa Salapaka¶
University of Illinois at Urbana-Champaign, Urbana, IL, 61801

This paper addresses a pivotal challenge in Unmanned Aerial Vehicle (UAV) networks crucial for sectors including delivery services, agriculture, and emergency response: optimizing UAV charging strategies for continuous operation in monitoring and inspection missions. We introduce a novel Maximum Entropy Principle (MEP) framework that employs mobile charging vehicles (MCVs), potentially Unmanned Ground Vehicles (UGVs), for in-field UAV charging. This MEP framework marks a significant advancement in the field by providing an integrated solution for multi-objective problems, including simultaneous obstacle-aware path planning and resource management under energy limitations. Distinguished from traditional heuristic approaches, our framework adeptly handles complex scenarios, significantly reducing optimization variables and facilitating robustness analysis. Through comprehensive simulations, our methodology has demonstrated significant advantages over existing algorithms in handling complex operational scenarios. Unlike other algorithms, which often struggle with large network sizes or intricate constraints, our solution consistently delivers robust performance. Empirical evidence indicates that our method achieves more than double the cost-effectiveness compared to its counterparts, coupled with multiple orders of magnitude faster operational speed. This research not only contributes to the theoretical understanding of autonomous UAV/UGV network planning but also has significant practical implications for real-time, field-deployable solutions.

I. Nomenclature

M	=	Total number of UGVs
N	=	Total number of UAVs
O	=	The set of all obstacles
f_j	=	UGV id
v_i	=	UAV id
δ_i	=	UAV destination id
x_i	=	Initial UAV deployment coordinates
y_j^0	=	Initial UGV deployment parameters
y_j	=	$r-$dimensional vector of UGV parameters to be optimized
z_i	=	UAV destination coordinates
K	=	Maximum number of stages

*Corresponding Author
†Ph.D. Candidate, Department of Mechanical Science and Engineering, University of Illinois at Urbana-Champaign.
‡Ph.D. Student, Department of Mechanical Science and Engineering, University of Illinois at Urbana-Champaign.
§Assistant Professor, Department of Computer Science and Engineering, University of Nevada, Reno.
¶Professor, Department of Mechanical Science and Engineering, University of Illinois at Urbana-Champaign.

$\eta_j^i(k)$ = Binary decision variable for UAV v_i to transition to waypoint f_j in the k^{th} step
ρ_i = Operation priority weight of UAV v_i
$l^i(k)$ = Waypoint id of UAV v_i at step k
c_0^i = Initial charge of UAV v_i
$c^i(k)$ = Charge of UAV v_i at step k
$R^i(c)$ = Range of UAV v_i with a battery charge c
$R^i(1)$ = Full Charge Range (F.C.R.) of UAV v_i
$d(\cdot,\cdot)$ = Distance function between two spatial waypoints
$\zeta^{\text{o}}(\cdot,\cdot)$ = Obstacle-aware penalty function between two waypoints, for the obstacle o
$D^i(k)$ = Total transition cost incurred by UAV v_i until step k
α = UGV cost factor
C_{UGV} = Transportation cost of UGVs
Γ_k = Stage k representing the set of all possible waypoints for UAVs
γ_k = An element (node) of stage Γ_k
γ = Path of a UAV modelled as an ordered tuple of the elements from the stages Γ_k
$\mathcal{G}$ = The set of all possible paths of the form γ taken by UAVs
$d_k^i(\cdot,\cdot)$ = Transition cost incurred by a UAV in moving from a facility in Γ_k to another facility in Γ_{k+1}
y_{γ_k} = Location/parameters corresponding to the facility represented by the value of $\gamma_k, \forall k$
$\eta^i(\cdot)$ = Binary decision variable to indicate the path taken by a particular UAV
$p^i(\cdot)$ = Probabilistic decision variable to indicate the probability of a path taken by UAV v_i
$p_k^i(\cdot|\cdot)$ = Probability of transition of v_i in stage k from one facility in Γ_k to another in Γ_{k+1}
H = Total entropy of distribution over the set of all the paths taken by all the UAVs
D = Cumulative cost incurred by all the UAVs
F = Free energy function
β = The annealing parameter

II. Introduction

Unmanned aerial vehicles (UAVs) are experiencing rapid advancements in technology, leading to a wide range of prospective civil applications. In recent years, the realm of UAVs has witnessed transformative advancements, especially in artificial intelligence and machine learning, fostering significant improvements in autonomous decision-making and operational efficiency. This evolution is particularly evident in the widespread adoption of UAVs for delivery services, which is revolutionizing supply chain dynamics and customer experiences. Presently, UAV networks are extensively employed in numerous sectors, including construction site monitoring, agricultural surveillance, environmental assessment, search and rescue missions, delivery logistics, data acquisition, and wireless communication [1]. These applications frequently entail intricate optimization and planning challenges, such as strategically locating facilities through facility location problems (FLPs) [2], [3], path planning [4], [5], and efficiently managing vehicle routing problems (VRPs) [6], [7]. Such optimization is also crucial for ensuring safety and regulatory compliance, given the limited range and endurance of UAVs. Additionally, as UAV networks expand in complexity and scale, optimal decision-making becomes imperative to manage and coordinate multiple UAVs effectively, thereby facilitating adaptability and responsiveness in dynamic environments. This approach not only bolsters operational effectiveness but also contributes to minimizing the environmental impact of UAV operations.

The mentioned optimization challenges usually appear as mixed-integer programming problems which are characterized by a large number of decision variables, non-convexity, and the presence of multiple local minima. Conventional heuristics-based approaches often yield suboptimal solutions, as their performance heavily relies on the initial conditions.

This paper introduces and validates a comprehensive framework, based on the Maximum Entropy Principle (MEP), that effectively handles various planning and logistics challenges in UAV networks. Our approach improves upon traditional models by offering a solution that can address a wide range of problems and constraints. For example, it efficiently manages UAV routes and resource allocation by planning the sequence of waypoints and allocating resources for tasks like service facility coverage. Additionally, the framework is carefully crafted to control traffic density, reducing congestion risks. It also optimizes UAV speed for better energy efficiency, timely mission completion, and reliability under uncertain conditions. This system strikes a fine balance between achieving optimal results and maintaining robustness, ensuring operational efficiency without sacrificing adaptability to changing situations. It takes into account

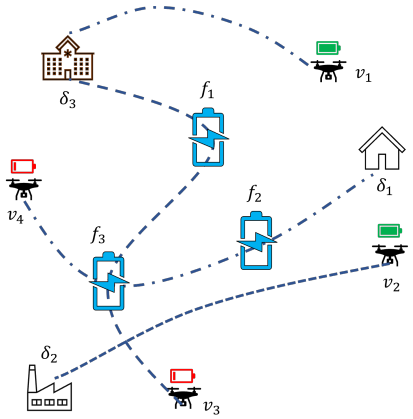

Fig. 1 Diagrammatic Representation of the Problem Overview.

various limitations, capacities, and geographical factors, making it a versatile tool for managing the complexities of UAV traffic.

The problem statement of this paper posits a network of UAVs, each with a predefined battery capacity and initial charge, along with charging Unmanned Ground Vehicles (UGVs), and a multitude of destination targets (see Fig. 1). This problem construction is inspired by real-world challenges in UAV operations, where the need for efficient charging strategies is paramount. Researchers have demonstrated the feasibility of long-term off-the-grid surveillance missions using self-sustainable UAVs and have explored ground charging infrastructure deployment. Moreover, the utilization of mobile charging vehicles (MCVs), including UGVs, has introduced innovative possibilities for field recharging, enabling complex coordination between UAVs and UGVs in energy-constrained environments. The primary objective is to design the flight paths in such a manner that minimizes the total weighted distance traversed by the UAVs, while ensuring that each UAV reaches its destination without exhausting its charge while avoiding all potential obstacles. The strategy involves a decision-making process where vehicles may either fly directly to their destination or via a network of charging UGVs, based on their deployment coordinates and the intended endpoint. This operational framework is designed to answer three pivotal questions: 1) What is the minimum number of charging nodes required to guarantee the feasibility of the UAVs' journeys? 2) What is the optimal route for each UAV, considering the need to balance expediency with energy conservation? 3) Where should the charging facilities be located to provide maximal support to the UAV fleet? Addressing these queries is essential to refine the efficiency and reliability of UAV operations within the proposed traffic management system. The upcoming sections detail our framework's systematic approach to answering these questions simultaneously, highlighting its comprehensive methodology and practical applications.

The results from multiple carefully designed simulations highlight our framework's proficiency in identifying optimal solutions that adhere to both UAV/UGV combined energy efficiency and obstacle avoidance requirements. Most importantly though, our approach significantly outperforms standard algorithms typically employed for such optimization problems, exhibiting superiority in terms of final cost efficiency, execution speed and ability to handle complicated scenarios. This contribution novelty is especially significant to facilitate real-time deployable solutions in the field with real autonomous UAV & UGV systems, which is a key consideration of our developed framework, as also discussed in the following sections.

III. Background and Literature Gap

Recent works have shown various approaches to multi-objective optimization in UAV networks. Some focus on secure communications at the physical layer through collaborative beamforming, emphasizing the challenges of ensuring security in UAV communications [8]. Others propose optimizations for maximizing data rates, energy harvesting, and minimizing UAV energy consumption over mission periods [9]. In multi-UAV systems, optimization problem formulations concerning parameters like energy, detection time, risk, and information gain have been explored, particularly in search and rescue applications [10]. This field is rich with problems and solutions involving mission completion time, signal strength, and total energy cost minimization in UAV swarm-assisted IoT applications [11].

Charging strategies in UAV networks are critical for continuous operations, especially in monitoring and inspection

missions. It has been demonstrated successfully that long-term deployments in wide-area airborne surveillance missions completely off-the-grid is possible through self-sustainable autonomous UAVs that can perform multiple back-to-back solar recharging cycles [12]. However, to facilitate even faster UAV recharging cycles, we may also assume some pre-established ground infrastructure in areas of interest; for instance certain studies propose deployment strategies for UAVs to maximize coverage of target areas while ensuring energy replenishment at ground charging stations [13]. Further progress in the state-of-the-art has unlocked advanced capabilities, but also higher challenges, by using MCVs –which could be UGVs– to provide charging support to UAVs in the field [14]. These may range from traditional UGVs with their known limitations, to novel versatile legged-locomotion systems that may navigate unstructured terrain while ferrying and simultaneously fast-recharging the UAV systems onboard reliably [15]. More importantly, it has been demonstrated that autonomous coordination of such marsupial UGV & UAV systems in the field can be successful, with multiple take-off and subsequent regrouping (UAV-UGV docking & fast-recharging) cycles becoming possible and being resiliently executed, even without wireless communication between agents, through the utilization of Deep-Learned strategies for airborne detection and autonomous vision-based guidance [16]. Futher works in the field of persistent surveillance with energy-constrained UAVs have also suggested mobile charging stations mounted on UGVs; these principally enable UAVs to recharge as they are transported to different locations [17]. A study proposed a UGV-UAV hybrid system where UGVs serve as moving charging stations for UAVs. In this setup, goods collected at a depot are delivered to the destination through UGVs and UAVs, with UGVs providing charging support for UAVs en route to their target points [18].

The incorporation of Artificial Intelligence (AI) in UAV routing protocols has gained attention, with trends leaning towards AI-enabled predictive networking and self-adaptive learning-based protocols [19]. Various routing algorithms have been proposed, including low latency routing algorithms based on partial location information and network connectivity [20]. Multi-agent reinforcement learning has also been utilized to aid dynamic routing in UAV swarm networks [21]. Power-Aware Routing (PAR) is another recent algorithm that considers adjustable power in UAV networks, aiming to find efficient transmission paths [22]. The autonomous navigation and obstacle avoidance capabilities of UAVs in uncharted territories are crucial for tasks such as geographical reconnaissance, cartography, field rescue operations, among others [23]. Research has also been directed towards autonomous obstacle avoidance based on obstacle contour detection, employing algorithms like the D* algorithm for path planning [24].

The growth of smart devices and reliance on cellular technologies have paved the way for UAV-enabled mobile edge computing, yet challenges like computation delay, transmission delay, and monetary cost remain. Distributed computation offloading schemes have been proposed to address challenges like low offloading efficiency, high energy consumption, and high complexity in UAV-enabled edge computing. The field is moving towards joint optimization of UAV trajectory, computation offloading, resource allocation, and machine-learning-driven optimization to handle these challenges [25, 26].

The academic landscape demonstrates a considerable volume of research dedicated to various planning problems, each typically treated as a distinct challenge. However, the convergence of these issues, especially within the realm of spatial networks, is notably under-researched. This gap in existing literature is due to the scarcity of studies that simultaneously tackle multiple planning and logistics challenges. The approaches in literature that involve multi-fold objectives often simplify the problem, making it more tractable for a metaheuristic algorithms like evolutionary or swarm-based algorithms. Simultaneously optimizing both the charging node locations and the exact routes for each vehicle significantly increases the complexity, as it involves a mix of continuous (node locations) and discrete (route waypoints) optimization; The complexity intensifies further when various network constraints are present.

In our prior research, we have made seminal contributions to this specialized field. The methodology proposed in [27] forms the cornerstone of our current research, aimed at addressing diverse planning problems in the context of UAV traffic management (UTM). This approach utilizes MEP from Statistical Physics, providing a notable benefit in reducing the quantity of variables that need to be optimized in such planning problem scenarios. This framework was selected due to its robust capability to integrate various constraints such as capacity, inclusion/exclusion criteria, and uncertainties in different parameters. Additionally, it offers a comprehensive platform for addressing a multitude of problems without restricting the algorithm's structure to a particular scenario. We posit that these attributes render the [27] framework eminently suitable for adaptation to UTM planning challenges, subject to requisite modifications.

IV. Network Configuration

The Unmanned Air Systems (UAS) that operate within this traffic management framework are diverse and multi-faceted, representing a heterogeneous fleet with varied capabilities and performance metrics. Each vehicle is designed

Fig. 2 Indicative illustration of our team's autonomous self-sustainable UAVs with solar and external-battery-powered recharging capabilities, and legged-locomotion UGVs that carry Docking-&-Recharging backpacks, allowing for their combined marsupial operation as Systems-of-Systems that can support wide-area deployments in-the-wild. Such classes of systems comprise the main paradigm considered as the target application field for this paper's proposed framework.

to operate at multiple speeds, catering to the broad spectrum of operational requirements. To facilitate efficient traffic management, these vehicles autonomously provide a suite of their own parameters to the central aggregator. These parameters include, but are not limited to, their points of origin and destination, energy levels, make and model, as well as critical travel parameters such as the desired estimated time of arrival (ETA). Moreover, they possess the functionality to report real-time path conditions back to the aggregator, ensuring the system remains abreast of the current traffic situation. In turn, the aggregator dispatches control parameters to each UAS, which are imperative for the vehicles to adhere to their assigned paths and schedules, thus maintaining an orderly and synchronized flow within the airspace.

Ground resources in our traffic management ecosystem are envisaged as a network of service stations (static) and UGVs that offer vital support services to the UAV fleet, primarily focusing on offering mobile recharging. The strategic positioning of these ground resources can maximize the accessibility of UAVs to in-situ recharging or other maintenance services. Moreover, their positioning is characterized by heterogeneity, since mobile UGVs can be redeployed dynamically to cater to the on-demand service needs of UAVs. Indicatively, especially marsupial solutions that combine UAVs with quadruped UGVs [16] which are known to exhibit high degrees of locomotion versatility [28], offer a particularly wide envelope of fleet deployment flexibility, unlocking operation across diverse locations and extending the UAVs' range by minimizing downtime and ensuring that they can quickly return to their designated flight paths (see Fig. 2). Through intelligent integration with the traffic management system, these ground resources serve as critical waypoints that enhance the overall robustness and reliability of the UAS network.

V. Mathematical Formulation

In building our analytical model, we establish several foundational assumptions to ground the framework. The initial deployment positions of the UAVs and their intended destinations are fixed within a Cartesian coordinate system, and they transit between the UGV service points to reach their destinations. Essentially, UGVs serve as the waypoints facilitating UAV transition within the network from their initial locations to their destinations in a sequential manner. We consider N UAVs in the network, indexed as $v_i, 1 \leq i \leq N$ with their initial locations at $x_i \in \mathbb{R}^2, 1 \leq i \leq N$. We denote UAV destinations by $\delta_i, 1 \leq i \leq N$, fixed at $z_i \in \mathbb{R}^2, 1 \leq i \leq N$. Further, we assume there are M UGVs indexed as $f_j, 1 \leq j \leq M$. The actions of UAVs are defined by the decision variables, $\eta_j^i(k) \in \{0,1\}^{N \times M \times K}, i \in \{1,2,\ldots,N\}, j \in \{1,2,\ldots,M\}, k \in \{1,2,\ldots,K\}$, where $\eta_j^i(k) = 1$ indicates that UAV v_i occupies UGV f_j in the k^{th} stage, otherwise $\eta_j^i(k) = 0$. Thus, the sequence $\{\eta_j^i(k), 1 \leq j \leq M\}_{k=1}^K$ determines UAV paths $\forall v_i$. We also denote the parameters associated with the UGVs, $y_j \in \mathbb{R}^{M \times r}, \forall j \in \{1,2,\ldots,M\}$ for which the network needs to be optimized, e.g., UGV coordinates, UAV schedules at UGVs, or similar parameters. In this paper, we focus on optimal placement of UGVs and optimal routing of the UAVs through them to their designated destinations.

UAVs are attributed varying degrees of operational priority $\rho_i \in [0,1], \sum_i \rho_i = 1$, allowing for the calibration of certain UAV types in alignment with their strategic importance. The charge levels c_0^i and $c^i(k), \forall k$ of each UAV are expressed as a value within the continuum from zero to one, denoting a scale from fully depleted to fully charged.

The Full-Charge-Range (F.C.R.) of a UAV is a critical metric indicating the maximum distance it can cover when fully charged, with the UAV's actual range being a direct linear function of its current charge level. We assume that UAVs are fully recharged upon visiting any charging nodes within the network, resetting their available range for continued operation. The associated UAV transition cost $d(\cdot,\cdot)$ between waypoint coordinates is defined by the spatial distance, and could be any valid distance function as deemed appropriate for the model's fidelity and computational efficiency. The transition cost may also include transition penalties incurred by the UAVs, for instance, due to range constraints, and obstacle-aware penalties. The cumulative cost $D^i(k)$ of a UAV's route is computed as the sum of these transitional distances, a factor which is subject to modification based on the specific requirements. Our goal is find an optimal coordinates for the $r-$dimensional UGV locations $y_j \in \mathbb{R}^r$ when initially located at $y_j^0 \in \mathbb{R}^r$ and optimal routes determined by $\eta_j^i(k)$ for all the UAVs such that the total UAV and UGV transportation cost in the network is minimized. These assumptions are integral to the formulation and subsequent optimization of the UAV traffic management system, providing a structured foundation from which the model can be elaborated and refined.

Hence, the problem is formulated as follows (refer to the **Nomenclature** for complete parameter definitions):

$$\min_{\eta,y} \sum_i \rho_i D^i(K) + \alpha \sum_j \|y_j - y_j^0\|^2 \tag{1}$$

$$\text{Subject to} \quad l^i(0) = l_0^i \quad \forall i \tag{2}$$

$$l^i(k) = l_d^i \quad \forall i, k \geq K \tag{3}$$

$$l^i(k+1) = \sum_{j=1}^{M} \eta_j^i(k) l_j \quad \forall i, k \quad l_j \in \{1, \ldots, M\} \tag{4}$$

$$D^i(0) = 0 \quad \forall i \tag{5}$$

$$D^i(k+1) = D^i(k) + d^*(l^i(k+1), l^i(k)) \quad \forall i, k \tag{6}$$

$$R^i(c^i(k)) \geq d^*(l^i(k+1), l^i(k))) \quad \forall i, k \tag{7}$$

$$\text{where:} \quad d^*(\cdot,\cdot) = d(\cdot,\cdot) + \sum_{o \in O} \zeta^o(\cdot,\cdot)$$

We pose the problem formulation from (1) to (7). In the formulation, the objective function (1) integrates two pivotal factors: the weighted sum of the total transition cost incurred by all the UAVs and the collective transportation cost of all the UGVs involved in relocating from their initial deployed positions y_j^0 to their optimized locations y_j. The cost function, C_{UGV}, is defined by the eq. $C_{\text{UGV}} = \alpha \sum_j \|y_j - y_j^0\|^2$, where α denotes the UGV cost factor. By quantifying this aspect, the model ensures a holistic optimization that minimizes not just the aerial paths of UAVs but also the ancillary costs associated with ground support logistics. The objective is to minimize the total cost function across the discrete-binary decision variables $\eta_j^i(k)$ and the spatial coordinates of UGVs, denoted as $y_j \in \mathbb{R}^r$, thereby formulating a mixed-integer programming problem.

The formulation incorporates constraints, such as (2) and (3), specifying the initial and final locations of all UAVs. Additionally, constraint (4) dynamically updates the waypoint location of UAVs during transitions through UGVs. The cumulative costs for each UAV are initialized and iteratively updated in accordance with constraints (5) and (6), respectively. This cost is adjusted by incorporating geometric distances and supplementary penalties to mitigate obstacles and accommodate for limited UAV charge range. Constraint (7) ensures that each transition between waypoints adheres to the prescribed charge limit for the UAVs.

VI. Proposed Solution

A. Intro to the Framework

In this section we adapt a sequential viewpoint to formulate and solve the formulation proposed in the previous section. This framework treats the problem as a sequential decision-making process and applies the Maximum Entropy Principle to handle its inherent complexity, known as $\mathcal{NP}$-hardness which arises due to simultaneous need to tackle facility location and routing problems. We also discuss practical constraints in detail, such as the limited range of the UAVs and obstacle aware penalties.

We view the multi-hop motion of each UAV in a sequential manner consisting of $M+2$ stages

$$\Gamma_0, \Gamma_1, \ldots, \Gamma_M, \Gamma_{M+1}.$$

The stage Γ_0 represents a UAV in its initial deployment location, $\Gamma_0 = \{v_i\}$ in their initial location. For $1 \leq k \leq M$, the stages Γ_k consist of all the charging nodes and the destinations $\Gamma_k = \cup_j \left\{f_j\right\} \cup \cup_i \{\delta_i\}$ and the final stage only consists of the destinations, $\Gamma_{M+1} = \cup_i \{\delta_i\}$.

We model the transportation path of a UAV $v_i \in \Gamma_0$ to its destination $\delta_i \in \Gamma_{M+1}$ through charging nodes as $\gamma = (\gamma_1, \gamma_2, \ldots, \gamma_M)$ where $\gamma_k \in \Gamma_k, \forall 1 \leq k \leq M$. If a UAV reaches its destination in stage Γ_q for some $q \leq M$, then $\gamma_k = \delta_i, q \leq k \leq M$. Let $\mathcal{G} := \{(\gamma_1, \ldots, \gamma_M) \ : \ \gamma_k \in \Gamma_k, 1 \leq k \leq M\}$ denote the set of all possible paths. For each path $\gamma \in \mathcal{G}$ taken by a UAV v_i, there is a transportation cost given by $d^i(\gamma) = \sum_{k=0}^{k=M} d_k^i(\gamma_k, \gamma_{k+1})$, where $d_k^i(\gamma_k, \gamma_{k+1})$ represents the transition cost incurred by UAV v_i in stage transition $\Gamma_k \rightarrow \Gamma_{k+1}$. In case of a simultaneous resource allocation and routing problem, the transition cost is determined by the geometrical distance between two consecutive waypoints γ_k and γ_{k+1}, which can take any valid distance function. In this paper, we have chosen Euclidean distance as an example, i.e. $d_k^i(\gamma_k, \gamma_{k+1}) = \|y_{\gamma_k} - y_{\gamma_{k+1}}\|$, where $y_{\gamma_k}, \forall k$ represents the location coordinates of UGV γ_k selected by UAV v_i in the Γ_k stage. Additionally, the transition cost accounts for penalties due to limited UAV charge range and obstacles in the paths (discussed in the subsection VI.B).

We formulate a Facility Location and Path Optimization (FLPO) problem which has two-fold objectives - finding an optimal path $\gamma \in \mathcal{G}$ for each $v_i, i \in \{1, 2, \ldots, N\}$ and optimal locations y_j for each facility $j \in \{1, 2, \ldots, M\}$. If $\eta^i(\gamma) \in \{0, 1\}$ is a binary association that represents the choice of the path γ that leads to minimum cost $d^i(\gamma)$, taken by v_i, then we intend to solve the following two-fold objective optimization

$$\begin{aligned} \min_{\{y_j\}} D &:= \min_{\{y_j\}} \sum_{v_i} \rho_i \sum_{\gamma \in \mathcal{G}} \eta^i(\gamma) d^i(\gamma) + \alpha \sum_j \|y_j - y_j^0\|^2 \\ \eta^i(\gamma) &= 1, \text{ if } \gamma = \arg\min_{\gamma \in \mathcal{G}} d^i(\gamma) \\ &= 0, \quad \text{otherwise.} \end{aligned} \tag{8}$$

Note that the above objective is same as that proposed in (1), except that the decision variables η and costs $d(\cdot)$ are defined over a space $\mathcal{G}$ of all possible paths γ. It is also crucial to note that this objective differs from standard FLPO problems due to the additional cost consideration for the transportation of UGVs. The above optimization problem requires solving for two coupled objectives as the cost of transportation $d^i(\gamma)$ for each v_i depends on both the path γ taken and the corresponding UGV locations $y_j, j \in \{1, 2, \ldots, M\}$ appearing in the path γ. One way to tackle the above coupled objective optimization problem is to solve each objective sequentially - first optimizing the locations of UGV charging nodes using a facility location algorithm and then determining the shortest transportation paths for UAVs to their destinations through a network graph. However, this method overlooks the interdependence of the objectives and its highly non-convex nature, leading to a suboptimal solution due to initialization biases. The solution approach adopted from [27] relaxes the choice of binary association variables $\eta^i(\gamma)$ with probability association variables $p^i(\gamma) \in [0, 1]$, $\sum_{\gamma \in \mathcal{G}} p^i(\gamma) = 1$. These probability associations now represent a p.m.f. over the space of all the paths $\mathcal{G}$ for each UAV v_i. This translates our objective of finding an optimal binary variables to finding optimal weights to each path assigned, making it "less commital" initially to any path chosen by a UAV. The optimal associations are determined by maximizing the *Shannon's entropy* of the distributions at fixed values of relaxed cost D_0

$$\begin{aligned} \max_{\substack{p^i(\cdot), \forall i \\ y_j, \forall j}} H &:= \max_{\substack{p^i(\cdot), \forall i \\ y_j, \forall j}} -\sum_i \rho_i \sum_{\gamma \in \mathcal{G}} p^i(\gamma) \log p^i(\gamma) \\ \text{Subject to } D &= \sum_i \rho_i \sum_{\gamma \in \mathcal{G}} p^i(\gamma) d^i(\gamma) + \alpha \sum_j \|y_j - y_j^0\|^2 = D_0. \end{aligned} \tag{9}$$

Note that for the hard probability associations i.e., $p^i(\gamma) = \eta^i(\gamma)$, the cost function D in (9) is identical to the original cost in (8). In this case, the coupled objective (8) has multiple local minima and the solution depends on the initial facility locations $y_j, \forall j$. Thus, to get rid of the local influence on the initialization condition, we first construct the following Lagrangian

$$\min_{\{y_j\}, p(\cdot|\cdot)} F := D - \frac{1}{\beta} H, \tag{10}$$

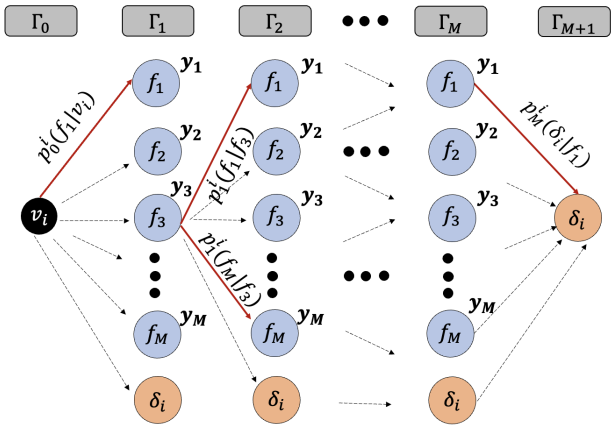

Fig. 3 Proposed FLPO framework.

also referred to as *free energy* adopted from the Statistical Physics analogy. The Lagrangian parameter β (also called as annealing parameter) is varied from zero to infinity, and analysis shows that decreasing D_0 is same as increasing β. The similar process in Statistical Physics, where the parameter "temperature" is decreased gradually is well known as "annealing". At small β, the entropy term H dominates and the objective is convex with respect to path probabilities $p^i(\gamma)$. The optimal solution leads to a uniform distribution $(p^i(\gamma))^* = 1/|\mathcal{G}|, \forall i$ over the set of all paths and a single facility location y_j^* at the centroid of all the initial UAV locations x_i. The value of β is incremented and the previous optimal solution is used an initial condition to solve the optimization problem (10) again. As we iterate at higher values of β, more weight is given to the minimization of D and optimal solution keeps tracking the global minima obtained in the first iteration. As $\beta \to \infty$, the probability associations converge to a binary association and we converge to the original problem (8).

Our framework's key strength lies in its ability to automatically provide binary solutions for path parameters at the end of the optimization process. This is done while only using continuous decision variables, avoiding the complexities of mixed-integer optimization. This unique feature gives our framework a significant advantage in solving complex problems that include binary variables, distinguishing it from other algorithms. We obtain our solution at larger values of β (or smaller values of D_0) starting with initial unbiased solution independent of initialization condition.

The sequential framework reduces the problem size by applying the law of optimality on the optimal transportation paths. It follows that the upcoming facility on the path is decided solely by the current facility and is independent of the prior facilities on that path. We impose this structure on our choice of the association weights $p^i(\gamma)$, which translates to a Markov property. Thus, the association weight $p^i(\gamma)$, which relates an entire transportation path $\gamma = (\gamma_1, ..., \gamma_M)$ to the UAV v_i, can be broken down into association weights $\{p_k(\gamma_{k+1}|\gamma_k)\}_{k=1}^M$, where $p_k(\gamma_{k+1}|\gamma_k)$ relates the stage Γ_k to Γ_{k+1} with $p_M^i(\delta_i|\gamma_M) = 1$ and initial transition probability denoted by $p_0^i(\gamma_1|v_i)$, more specifically $p(\gamma|\gamma_0) = \Pi_{k=0}^M p_k(\gamma_k|\gamma_0)$ (see Fig. 3). Since the Lagrangian F is convex with respect to $p_k^i, \forall i, k$, setting $\frac{\partial F}{\partial p_k^i} = 0, \forall i, k$ yields

$$p_k^i(\gamma_{k+1}|\gamma_k) = e^{-\beta d_k^i(\gamma_k,\gamma_{k+1})} \frac{\sum_{\substack{(\sigma_{k+2},...,\sigma_M):\\ \sigma_{k+1}=\gamma_{k+1}}} e^{-\beta \sum_{t=k+1}^M d_t^i(\sigma_t,\sigma_{t+1})}}{\sum_{\substack{(\sigma_{k+1},...,\sigma_M):\\ \sigma_k=\gamma_k}} e^{-\beta \sum_{t=k}^M d_t^i(\sigma_t,\sigma_{t+1})}}. \tag{11}$$

Therefore, we can directly compute path parameters using (11), leaving only y_j to be solved. This separation significantly reduces computational complexity, as the quantity of y_js is considerably less than the number of path variables $p_k^i(\gamma_{k+1}|\gamma_k)$. Observing eq. (11), it becomes evident that as $\beta \to \infty$, the path variables $p_k^i(\gamma_{k+1}|\gamma_k)$ converge to one for segments on the shortest path from a given node, and zero elsewhere. Substituting the above expression back in (10) gives an expression for free energy

$$F = -\frac{1}{\beta} \sum_i \rho_i \log \sum_{\gamma \in \mathcal{G}} e^{-\beta \sum_{t=0}^M d_t^i(\gamma_t,\gamma_{t+1})} + \alpha \sum_j \|y_j - y_j^0\|^2 \tag{12}$$

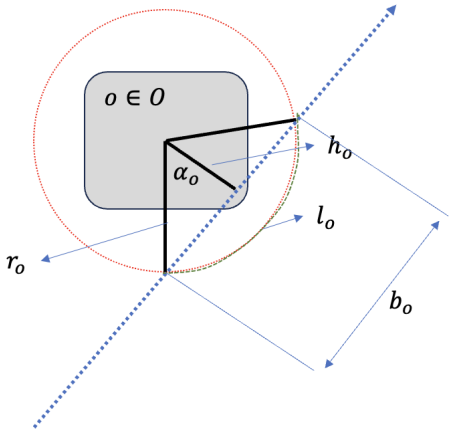

Fig. 4 Diagrammatic obstacle penalty model.

and further solving for $\frac{\partial F}{\partial y_j} = 0$ gives the optimal location of facilities at every β. Standard numerical optimization schemes can also be incorporated to to minimize the modified free energy function (12) over y_js.

B. Constraints and assumptions

The viability of a given scenario within our UAV traffic management framework is bound by specific feasibility criteria, which are chiefly governed by the costs associated with UAV transitions.

- **UAV Full Charge Range**: Any transition exceeding the UAV's current range incurs a prohibitively high cost, modeled by a hyperbolic tangent function that approaches infinity as the distance surpasses the UAV's capacity at that stage. Accordingly, the sequential transition cost function defined in the previous section is modified to

$$d_k^i(\gamma_k, \gamma_{k+1}) = \|y_{\gamma_k} - y_{\gamma_{k+1}}\| + \frac{\mu}{2}\left(\tanh\left[\|y_{\gamma_k} - y_{\gamma_{k+1}}\| - R^i(c^i(k))\right] + 1\right) \tag{13}$$

  where μ is a constant (typically a large value). While a transition may fall within the UAV's range, it might still be deemed inadvisable if it poses a substantial risk of battery depletion. The feasibility of a scenario is contingent upon various factors: the UAVs' initial coordinates, their intended destinations, the levels of initial charge, and the number of accessible charging nodes. In certain instances, the constellation of these parameters may render a scenario infeasible, with no solution that ensures all UAVs reach their destinations without exhausting their charge en route. Such infeasibility becomes evident upon examining the cumulative cost post-optimization termination. This metric serves as a simple diagnostic tool, enabling us to ascertain the requisite minimum number of charging nodes to render a scenario viable, providing a way to answer the first proposed research question addressed in the Introduction.
- **Obstacle Avoidance** : In the presented model, obstacle avoidance is incorporated into the UAV's route planning by adjusting the flight path to circumvent any potential obstructions within the airspace. When a UAV encounters an obstacle, the system calculates an alternative route—referred to as the corrected route—that skirts around the obstruction. For demonstration purposes only, we assume that obstacles are bound within circular areas that UAVs need to avoid (although our method is not dependant on this assumption). We denote the set of all obstacles by O. If an obstacle o $\in O$ with radius r_o intersects with a straight line path between γ_k and γ_{k+1}, as shown in Fig. 4, then UAVs circumvent the obstacle in an arc of length $l_o(\gamma_k, \gamma_{k+1})$ given by

$$l_o(\gamma_k, \gamma_{k+1}) = 2r_o \tan^{-1}\left(\frac{b_o(\gamma_k, \gamma_{k+1})}{\sqrt{4r_o^2 - b_o(\gamma_k, \gamma_{k+1})^2}}\right) \tag{14}$$

  where b_o is the portion of the straight line path intercepted inside the circle. The additional path length covered by UAV around obstacle o is given by $\zeta^o(\gamma_k, \gamma_{k+1}) = l_o(\gamma_k, \gamma_{k+1}) - b_o(\gamma_k, \gamma_{k+1})$ and the transition cost (13) is further updated as below

$$d_k^i(\gamma_k, \gamma_{k+1}) = \|y_{\gamma_k} - y_{\gamma_{k+1}}\| + \frac{\mu}{2}\left(\tanh\left[\|y_{\gamma_k} - y_{\gamma_{k+1}}\| - R^i(c^i(k))\right] + 1\right) + \sum_{o \in O} \zeta^o(\gamma_k, \gamma_{k+1}) \tag{15}$$

The additional term in the cost is summed over all the obstacles but it penalizes only for those obstacles which are intersected by line between γ_k and γ_{k+1}. If an obstacle $o' \in O$ does not intersect the path joining between γ_k and γ_{k+1}, then the additional cost is zero because $b_{o'} = 0 \Rightarrow l_{o'} = 0 \Rightarrow \zeta^{o'}(\gamma_k, \gamma_{k+1}) = 0$. This deviation from the original path is necessary to maintain safety and operational integrity. The model considers this detour by integrating the additional distance and complexity into the transition cost function of the UAV's journey. Therefore, the corrected route not only ensures avoidance of the obstacle but also reflects the associated cost implications of this avoidance in the UAV's flight plan optimization.

VII. Simulations and Results

The methodology of this paper is evaluated through a series of simulations over different scenarios. We will demonstrate the ability of this framework on finding the optimal location of UGVs, the optimal routes of UAVs to their destination coordinates, while satisfying combined energy demands as well as avoiding obstacles along their routes. The scenarios have been meticulously designed to provide a robust testbed, ensuring that all constraints are met under challenging conditions. While our framework has undergone testing on UAV networks with hundreds of units, we opted for a smaller UAV network to gain a deeper insight into the problem and its solution.

Fig. 5 presents the simulation results for four distinct scenarios, each introducing a unique complexity to the routing and facility location dimensions of the strategic planning problem. The simulation incorporates ten UAVs ($N = 10$) and three obstacles, where initial charge levels, deployment and destination coordinates for UAVs, and obstacle geographical characteristics across all scenarios are identical in all of the scenarios. For the purposes of this analysis, we presume a homogeneous UAV network with uniform F.C.R. and a standardized cost factor. These variables were deliberately selected to create a demanding context for locating charging nodes and determining optimal UAV pathways. The initial location, destination location, and initial charge level of the UAVs considered for simulations are as follows: ((10.0, 5.0), (45.0, 50.0), 0.7), ((3.0, 40.0), (50.0, 10.0), 0.5), ((20.0, 15.0), (35.0, 35.0), 0.6), ((5.0, 30.0), (25.0, 5.0), 0.4), ((40.0, 45.0), (10.0, 10.0), 0.8), ((30.0, 20.0), (5.0, 35.0), 0.6), ((15.0, 10.0), (40.0, 40.0), 0.4), ((35.0, 5.0), (10.0, 45.0), 0.5), ((25.0, 40.0), (20.0, 10.0), 0.7), and ((45.0, 15.0), (5.0, 20.0), 0.3).

In Fig. 5-a, the scenario is configured with three charging nodes ($M = 3$), revealing the absence of a viable coordination that ensures all UAVs retain sufficient energy. The optimization terminates with multiple UAVs depleting their energy reserves along their routes, indicating a necessity to augment the number of charging nodes. This adjustment is evidenced in Fig. 5-b ($M = 4$), where the optimization algorithm effectively meets the energy requirements against the backdrop of obstacles, simultaneously optimizing to reduce the aggregate average travel distance. Fig. 5-c illustrates the implications of reducing the UAVs' range by 10% form 25 to 22.5 on the strategic planning, resulting in a minor shift in charging node positioning coupled with a modification of UAV trajectories to sustain energy viability in the new setup. Finally, Fig. 5-d elucidates the impact of introducing a non-trivial cost for UGV transport distances on the preferential positioning of charging nodes($\alpha = 10$), skewing them towards their initial deployment coordinates, exemplified here as (25,50)—while concurrently satisfying obstacle-aware optimality and energy sufficiency in all path segments.

The annealing process within our framework is pivotal for enabling the algorithm to bypass local minima and approach solution spaces close to the global optimum. The parameter β, when varied from lower to higher values as per eq. (10), alters the cost function's landscape. Initially, at lower β values, the cost function, represented by a smoother and more manageable state, gradually transitions to the actual original cost D, as indicated in eq. (9). This original cost function is inherently more challenging to optimize due to its sharp transitions for minor variable changes and its minimal gradient over extensive areas between these transitions.

In simpler terms, starting with $\beta \approx 0$ implies beginning with a smoother cost function. By solving the optimization problem at this stage and progressively increasing β, we utilize the solution obtained for the preceding β value as the initial estimate for the subsequent β value. This strategy aids in maintaining proximity to the optimal solution throughout the transition to the more complex actual cost function. Fig. 6 illustrates how varying β impacts the cost function's shape, focusing on the optimization of four charging facility locations in scenario (b) from the preceding section. To produce these plots, we initially determined the optimal positions for facilities $F1 - F4$. Then, we varied each facility's location individually while keeping the others fixed at their optimal positions. The top four plots correspond to a small β value, showcasing a smoother cost function with substantial gradients across the domain. Conversely, the bottom four plots, associated with a large β value, reveal sharp transitions in proximity to the optimum locations and nearly zero gradients across most of the optimization domain. Consequently, in the latter scenario, pinpointing the optimal location poses a significant challenge for optimization algorithms.

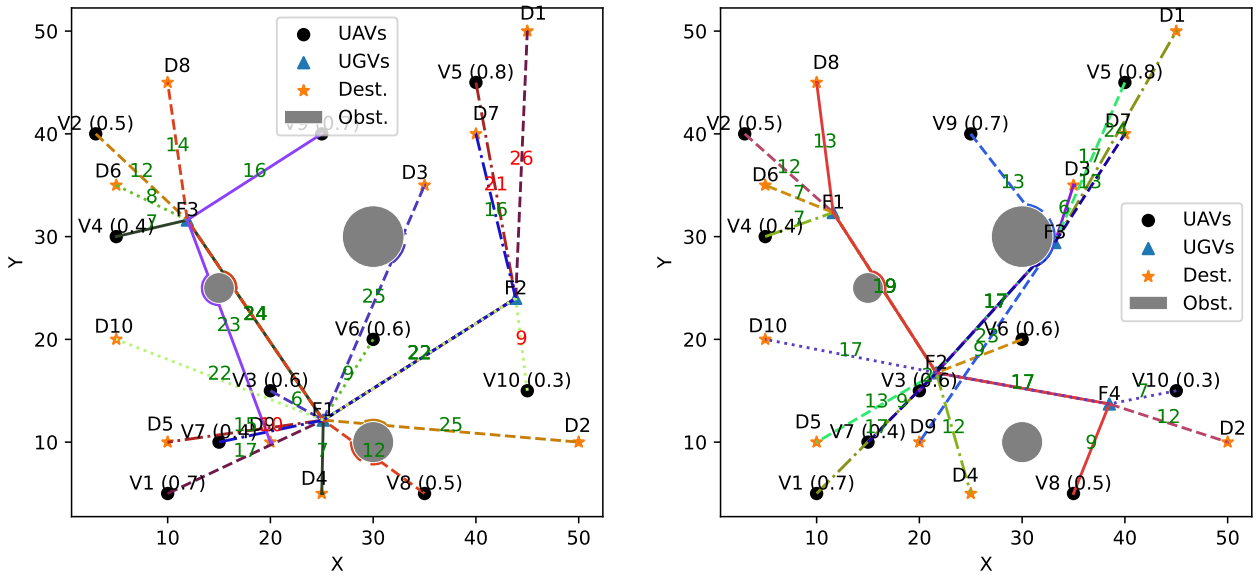

(a) $M = 3, F.C.R = 25, \alpha = 0$

(b) $M = 4, F.C.R = 25, \alpha = 0$

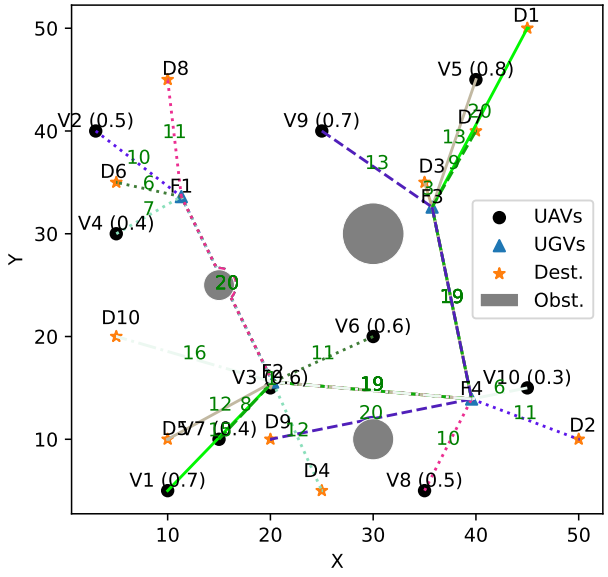

(c) $M = 4, F.C.R = 22.5, \alpha = 0$

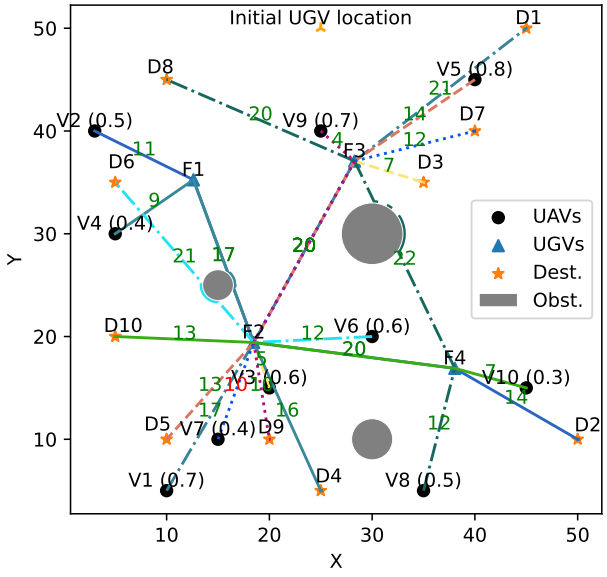

(d) $M = 4, F.C.R = 25, \alpha = 10$

Fig. 5 Results of the Simulation: The paths taken by the UAVs are differentiated using various colors and line styles. The length of each path segment is indicated by numerical values. Green numbers represent segments that fall within the UAV's operational range, while red numbers highlight segments where energy constraints are either borderline or violated.

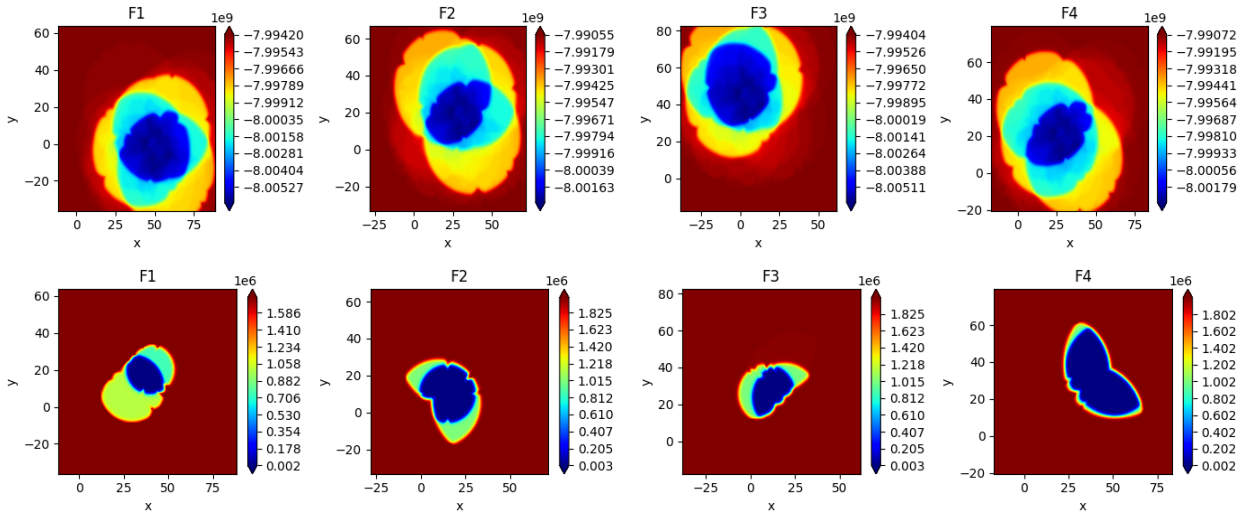

Fig. 6 Local variations of the free energy function (12) with respect to location of each charging node, for the second scenario in Fig. 5, at $\beta = 1e-8$ (top plots) and $\beta = 1e8$ (bottom plots).

A. Benchmark against standard algorithms

To compare the performance of our algorithm with other standard methodologies utilized in this domain, we have chosen three evolutionary algorithms to tackle the optimization problem proposed in this paper. These algorithms are: Genetic Algorithm (GA), Covariance matrix adaptation evolution strategy (CMA-ES), and Particle Swarm Optimization (PSO). The hyperparameters of these algorithms are provided in Table 1. The first two were implemented using the standard "DEAP"*, and the third using the "Pyswarms"† Python packages.

Our algorithm introduces a significant advancement in computational efficiency over existing methodologies. By integrating the Shannon entropy term into the MEP framework, we achieve a substantial reduction in the number of optimization variables. Specifically, the free energy function, as shown in eq. 12, depends solely on the facility locations $y_j : j \in \{1, \ldots, M\}$. This integration eliminates the need to optimize over route parameters $p_k(\gamma_{k+1}|\gamma_k)$, which can be directly computed using the Gibbs distribution (11). In contrast to other methods that aim to optimize a multi-faceted objective function (1), our approach significantly reduces computational complexity. This reduction is achieved by limiting the optimization variables to facility locations, whereas other methods must include both facility locations and route parameters for all UAVs. Consequently, our framework exhibits superior scalability for large-scale scenarios involving numerous UAVs and facilities, a capability that other methodologies find challenging to manage efficiently in comparably extensive problem setups.

To establish a meaningful comparison with alternative algorithms, we first simplified the original planning problem, as outlined in eq. 1. This simplification was necessary to adapt the problem for optimization by metaheuristic algorithms, which require meticulous customization for handling mixed-integer cost functions and their inherent constraints. For instance, genetic algorithms (GAs) necessitate tailored *mutation* and *crossover* operators to effectively manage mixed optimization variables. Recognizing that the performance of these algorithms can be significantly influenced by such modifications, we opted for a relaxed version of the cost function, denoted as D in eq. 9. In this relaxed model, all optimization variables are continuous. In our MEP framework, the number of optimization variables is rM in an r-dimensional setting. This contrasts with the $rM + N(M^2 + 1)(M + 1)$ parameters required by other algorithms when including route parameters. The disparity in variable count in the order of $\approx NM^3$, becomes substantial for large values of N and M, rendering the optimization of extensive UAV and facility networks nearly impractical with other algorithms.

Therefore, while our framework is capable of handling large-scale scenarios, we selected The first scenario in the previous section for benchmarking, with additional simplifications. To further align with the capabilities of other algorithms, we adjusted the UAV range ($F.C.R$) to 200. This adjustment not only simplifies the objective space but also eases the optimization challenge by reducing significant penalty terms related to energy violation constraints, thereby smoothing the cost function. In this case, all UAVs will have the capacity to go directly to their destinations, and no

*https://deap.readthedocs.io/en/master/

†https://pyswarms.readthedocs.io/en/latest/

Table 1 Hyperparameters of Genetic Algorithm, PSO Algorithm, and CMA-ES Algorithm

Algorithm	Parameter	Value
GA	Population Size	100
	Number of Generations	2000
	Crossover Probability (cxpb)	0.9
	Mutation Probability (mutpb)	0.25
	Selection Method	Tournament Selection
	Tournament Size	3
	Initialization Method	Random Uniform Distribution
PSO	Number of Particles	100
	Number of Generations	1000
	Topology Class	star
	C1 (Cognitive Weight)	0.2
	C2 (Social Weight)	0.8
	W (Inertia Weight)	0.95
CMA-ES	Number of Generations	3000
	Sigma (σ)	0.3
	Population Size (λ)	100
	Strategy	Derandomized Self-Adaptation

Table 2 Performance Metrics of Algorithms

Methodology	Mean Cost	CV Cost	Mean Time (s)	CV Time
Proposed method	401.982	0.000	4.748	0.212
GA	861.718	0.017	903.024	0.004
PSO	990.775	0.057	719.769	0.040
CMA-ES	1016.855	0.190	1680.674	0.003

re-charge is needed. The total cost in this case is almost equal to 400. Hence, we assess the capability of algorithms to find this obvious solution of this case.

Table 2 presents the results of simulations conducted for various algorithms. Each algorithm underwent three trials, with the results including the average (Mean) and the Coefficient of Variation (CV) for both cost and execution time[‡]. Notably, our algorithm swiftly identified the solution for this scenario, in stark contrast to the other algorithms, which remained trapped in local minima, taking significantly longer. This underscores the superior efficiency and effectiveness of our algorithm in addressing such optimization challenges.

B. Sensitivity Analysis

Sensitivity analysis emerges as a critical component of our framework, offering an insightful examination into how variations in network parameters—such as traffic volume, traffic density, UAS-type configurations, the number and type of UAV facilities, and the incidence of communication errors and delays—affect overall system performance. By systematically altering these parameters, our framework can predict and quantify the impact of each factor on the network's efficacy. This allows for informed decision-making and resource prioritization, ensuring that allocation is not only strategic but also adaptive to potential fluctuations within the system. Moreover, sensitivity analysis is indispensable for risk assessment and enhancing the resilience of the network. It empowers us to identify and fortify the network's vulnerabilities to external disturbances or operational changes, thereby bolstering the robustness of UAV

[‡]All of the algorithms are executed using an Intel® Core™ i7-4790 CPU (@ 3.60 GHz).

traffic management and safeguarding against disruptions that could otherwise compromise the integrity and reliability of UAV services.

To delve into sensitivity analysis, it is crucial to grasp how the free energy (10) behaves in relation to framework parameters, such as the location of the battery charging nodes, UAV full charge range, and size of the obstacles in between the paths. For instance, the derivative of the free energy F in (10) with respect to a facility location $y_r, \forall r \in \{1, 2, \ldots, M\}$ is given by

$$\frac{\partial F}{\partial y_r} = \sum_i \left[\frac{\partial F}{\partial d_0^i(v_i, \gamma_1^r)} \cdot \frac{\partial d_0^i(v, \gamma_{k+1}^r)}{\partial y_r} + \sum_{\gamma_2 \in \Gamma_2} \frac{\partial F}{\partial d_1^i(\gamma_1^r, \gamma_2)} \cdot \frac{\partial d_1^i(\gamma_1^r, \gamma_2)}{\partial y_r} \right.$$
$$\left. + \sum_{k=1}^{M-1} \left(\sum_{\gamma_k \in \Gamma_k} \frac{\partial F}{\partial d_k^i(\gamma_k, \gamma_{k+1}^r)} \cdot \frac{\partial d_k^i(\gamma_k, \gamma_{k+1}^r)}{\partial y_r} + \sum_{\gamma_{k+2} \in \Gamma_{k+2}} \frac{\partial F}{\partial d_{k+1}^i(\gamma_{k+1}^r, \gamma_{k+2})} \cdot \frac{\partial d_{k+1}^i(\gamma_{k+1}^r, \gamma_{k+2})}{\partial y_r} \right) \right] + 2\alpha(y_r - y_r^0) \tag{16}$$

where the waypoint $\gamma_k^r \in \Gamma_k, \forall k$ has the parameter y_r. The above expression has two terms, the first term is the result of UAV transportation and the second term is due to UGV transportation, which is linear in y_r. The first term has the derivatives of free energy and transition costs as unknowns. The derivative of the transition cost with respect to facility locations in the above expression can be computed explicitly in the following form

$$\frac{\partial d_k^i(s,t)}{\partial y_r} = \kappa_{s,r} \left(\frac{y_r - y_t}{\|y_r - y_t\|} \left(1 + 0.5 \text{sech}^2 \left(\|y_r - y_t\| - R^i(c^i(k)) \right) \right) + \sum_{o \in O} \frac{\partial}{\partial y_r} \zeta^o(r,t) \right)$$
$$+ \kappa_{t,r} \left(\frac{y_r - y_s}{\|y_r - y_s\|} \left(1 - 0.5 \text{sech}^2 \left(\|y_s - y_r\| - R^i(c^i(k)) \right) \right) + \sum_{o \in O} \frac{\partial}{\partial y_r} \zeta^o(s,r) \right), \forall s \in \Gamma_k, t \in \Gamma_{k+1} \tag{17}$$

where $\kappa_{u,v} = 1$, if $u = v$ and 0 otherwise, is Kronecker Delta function. Further, y_s and y_t are facility locations of the waypoints $s \in \Gamma_k$ and $t \in \Gamma_{k+1}$ and the node r has facility location y_r. The Gibbs distribution structure of the probability associations in (11) provides an interesting interpretation of the derivative of free energy with respect to transition cost.

Proposition 1 *For the transition $\Gamma_K \ni s \to t \in \Gamma_{K+1}$ for $K \in \{0, 1, 2, \ldots, M\}$, the gradient of free energy function F with respect to the transition cost $d_K^i(s,t)$ is equivalent to the probability that v_i reaches $t \in \Gamma_{K+1}$ stage through $s \in \Gamma_K$, i.e.*

$$\frac{\partial F}{d_K^i(s,t)} = \rho_i \sum_{\gamma_1, \ldots, \gamma_{K-1}} p_0^i(\gamma_1|v_i) p_1^i(\gamma_2|\gamma_1) \ldots p_{K-1}^i(s|\gamma_{K-1}) p_K^i(t|s) \leq 1 \tag{18}$$

Proof: See appendix 1

The equations (17) and (18) can be substituted into (16) to analyze the sensitivity of free energy with respect to facility locations. The above remark signifies that the free energy is "well-behaved" with respect to the transition cost function. The transition cost function can have discontinuous changes, for example, due to appearance of tan hyperbolic function, which applies large penalties to avoid any constraint violations (see subsection VI.B). Irrespective, the free energy does not change arbitrarily. Furthermore, the combinatorial sum over the set of all the paths passing through $s \in \Gamma_K$ to $t \in \Gamma_{K+1}$ can be calculated using a dynamic programming sum leading to efficient computation. Additionally, the sequential framework allows us to use matricization techniques for faster computation of free energy gradient and its efficient implementation.

VIII. Conclusion

In summary, this study presents a significant breakthrough in UAV network optimization with the development of an MEP framework for efficient UAV charging. Our approach surpasses existing methods in cost, speed, and complexity management, offering valuable insights for theoretical understanding and practical deployment in different sectors. Acknowledging the limitations in simulation scope, our future research will involve expanding this framework to encompass other aspects of UAV networks, such as scheduling and congestion at service facilities. Additionally, we plan to implement our framework in on-the-field trials with actual UAVs, further validating its effectiveness in real-world scenarios. This work not only advances UAV/UGV network planning but also paves the way for ongoing innovation in autonomous vehicle integration.

Appendix

Appendix 1 *Proof of proposition 1*

Proof : Differentiating F with respect to $d_K^i(s,t)$ for some $K \in \{0,1,\ldots,M\}$, some $s \in \Gamma_K, t \in \Gamma_{K+1}$

$$\begin{aligned}
\frac{\partial F}{\partial d_K^i(s_i,s_j)} &= -\frac{\rho_i}{\beta}\frac{\partial}{\partial d_K^i(s,t)}\log \sum_{\substack{\gamma_1,\gamma_2,\ldots,\gamma_M \\ \gamma_{M+1}=\delta_i}} e^{-\beta\sum_{k=0}^{M} d_k^i(\gamma_k,\gamma_{k+1})} \\
&= -\frac{\rho_i}{\beta}\frac{1}{\sum_{\substack{\gamma_1,\gamma_2,\ldots,\gamma_M \\ \gamma_{M+1}=\delta_i}} e^{-\beta\sum_{k=0}^{M} d_k^i(\gamma_k,\gamma_{k+1})}} \sum_{\substack{\gamma_1,\gamma_2,\ldots,\gamma_M \\ \gamma_{M+1}=\delta_i}} \frac{\partial}{\partial d_K^i(s,t)} e^{-\beta\sum_{k=0}^{M} d_k^i(\gamma_k,\gamma_{k+1})} \\
&= \frac{\rho_i}{\sum_{\substack{\gamma_1,\gamma_2,\ldots,\gamma_M \\ \gamma_{M+1}=\delta_i}} e^{-\beta\sum_{k=0}^{M} d_k^i(\gamma_k,\gamma_{k+1})}} \sum_{\substack{\gamma_1,\gamma_2,\ldots,\gamma_M \\ \gamma_{M+1}=\delta_i}} e^{-\beta\sum_{k=0}^{M} d_k^i(\gamma_k,\gamma_{k+1})} \sum_{k=0}^{M} \frac{\partial d_k^i(\gamma_k,\gamma_{k+1})}{\partial d_K^i(s,t)} \\
&= \frac{\rho_i}{\sum_{\substack{\gamma_1,\gamma_2,\ldots,\gamma_M \\ \gamma_{M+1}=\delta_i}} e^{-\beta\sum_{k=0}^{M} d_k^i(\gamma_k,\gamma_{k+1})}} \sum_{\substack{\gamma_1,\gamma_2,\ldots,\gamma_M \\ \gamma_{M+1}=\delta_i}} e^{-\beta\sum_{k=0}^{M} d_k^i(\gamma_k,\gamma_{k+1})} \sum_{k=0}^{M} \kappa_{k,K}\kappa_{s,\gamma_k}\kappa_{t,\gamma_{k+1}} \\
&= \frac{\rho_i}{\sum_{\substack{\gamma_1,\gamma_2,\ldots,\gamma_M \\ \gamma_{M+1}=\delta_i}} e^{-\beta\sum_{k=0}^{M} d_k^i(\gamma_k,\gamma_{k+1})}} \sum_{\substack{\gamma_1,\gamma_2,\ldots,\gamma_M \\ \gamma_{M+1}=\delta_i}} e^{-\beta\sum_{k=0}^{M} d_k^i(\gamma_k,\gamma_{k+1})} \kappa_{s,\gamma_K}\kappa_{t,\gamma_{K+1}} \\
&= \frac{\rho_i}{\sum_{\substack{\gamma_1,\gamma_2,\ldots,\gamma_M \\ \gamma_{M+1}=\delta_i}} e^{-\beta\sum_{k=0}^{M} d_k^i(\gamma_k,\gamma_{k+1})}} \sum_{\substack{\gamma_1,\gamma_2,\ldots,\gamma_M \\ \gamma_{M+1}=\delta_i \\ \gamma_K=s,\gamma_{K+1}=t}} e^{-\beta\sum_{k=0}^{M} d_k^i(\gamma_k,\gamma_{k+1})}
\end{aligned}$$

Since we have the probability associations obtained as Gibbs distribution in 11, we notice that the above expression can be written as a probability that at least one UAV performs the transition from $s \in \Gamma_K$ to $t \in \Gamma_{K+1}$

$$\begin{aligned}
\frac{\partial F}{\partial d_K^i(s,t)} &= \rho_i \sum_{\substack{\gamma_1,\gamma_2,\ldots,\gamma_M \\ \gamma_K=s,\gamma_{K+1}=t}} p_0^i(\gamma_1|v_i)p_1^i(\gamma_2|\gamma_1)\ldots p_{K-1}^i(s|\gamma_{K-1})p_K^i(t|s)p_{K+1}^i(\gamma_{K+1}|t)\ldots p_M^i(\delta|\gamma_M) \\
&= \rho_i \sum_{\gamma_1,\ldots,\gamma_{K-1}} p_0^i(\gamma_1|v_i)p_1^i(\gamma_2|\gamma_1)\ldots p_{K-1}^i(s|\gamma_{K-1})p_K^i(t|s)\cdot \\
&\qquad \sum_{\gamma_{K+1},\ldots,\gamma_M} p_{K+1}^i(\gamma_{K+1}|t)\ldots p_{M-1}^i(\gamma_M|\gamma_{M-1}) \\
&= \rho_i \sum_{\gamma_1,\ldots,\gamma_{K-1}} p_0^i(\gamma_1|\gamma_0)p_1^i(\gamma_2|\gamma_1)\ldots p_{K-1}^i(s|\gamma_{K-1})p_K^i(t|s) \le 1
\end{aligned} \tag{19}$$

Acknowledgments

We acknowledge the support of National Aeronautics and Space Administration under Grant NASA 80NSSC22M0070 for this work.

References

[1] Otto, A., Agatz, N., Campbell, J., Golden, B., and Pesch, E., "Optimization approaches for civil applications of unmanned aerial vehicles (UAVs) or aerial drones: A survey," *Networks*, Vol. 72, No. 4, 2018, pp. 411–458.

[2] Shavarani, S. M., Mosallaeipour, S., Golabi, M., and İzbirak, G., "A congested capacitated multi-level fuzzy facility location problem: An efficient drone delivery system," *Computers & Operations Research*, Vol. 108, 2019, pp. 57–68.

[3] Shavarani, S. M., "Multi-level facility location-allocation problem for post-disaster humanitarian relief distribution: a case study," *Journal of Humanitarian Logistics and Supply Chain Management*, Vol. 9, No. 1, 2019, pp. 70–81.

[4] Phung, M. D., Quach, C. H., Dinh, T. H., and Ha, Q., "Enhanced discrete particle swarm optimization path planning for UAV vision-based surface inspection," *Automation in Construction*, Vol. 81, 2017, pp. 25–33.

[5] Sancı, S., and İşler, V., "A parallel algorithm for UAV flight route planning on GPU," *International Journal of Parallel Programming*, Vol. 39, 2011, pp. 809–837.

[6] Gottlieb, Y., and Shima, T., "UAVs task and motion planning in the presence of obstacles and prioritized targets," *Sensors*, Vol. 15, No. 11, 2015, pp. 29734–29764.

[7] Jiang, X., Zhou, Q., and Ye, Y., "Method of task assignment for UAV based on particle swarm optimization in logistics," *Proceedings of the 2017 international conference on intelligent systems, metaheuristics & swarm intelligence*, 2017, pp. 113–117.

[8] Li, J., Sun, G., Kang, H., Wang, A., Liang, S., Liu, Y., and Zhang, Y., "Multi-Objective Optimization Approaches for Physical Layer Secure Communications Based on Collaborative Beamforming in UAV Networks," *IEEE/ACM Transactions on Networking*, Vol. 31, No. 4, 2023, pp. 1902–1917. https://doi.org/10.1109/TNET.2023.3234324.

[9] Yu, Y., Tang, J., Huang, J., Zhang, X., So, D. K. C., and Wong, K.-K., "Multi-Objective Optimization for UAV-Assisted Wireless Powered IoT Networks Based on Extended DDPG Algorithm," *IEEE Transactions on Communications*, Vol. 69, No. 9, 2021, pp. 6361–6374. https://doi.org/10.1109/TCOMM.2021.3089476.

[10] Yanmaz, E., "Joint or decoupled optimization: Multi-UAV path planning for search and rescue," *Ad Hoc Networks*, Vol. 138, 2023, p. 103018. https://doi.org/https://doi.org/10.1016/j.adhoc.2022.103018, URL https://www.sciencedirect.com/science/article/pii/S1570870522001901.

[11] Li, J., Sun, G., Duan, L., and Wu, Q., "Multi-Objective Optimization for UAV Swarm-Assisted IoT with Virtual Antenna Arrays," *IEEE Transactions on Mobile Computing*, 2023, pp. 1–18. https://doi.org/10.1109/tmc.2023.3298888, URL https://doi.org/10.1109%2Ftmc.2023.3298888.

[12] Carlson, S. J., Arora, P., Karakurt, T., Moore, B., and Papachristos, C., "Towards multi-day field deployment autonomy: A long-term self-sustainable micro aerial vehicle robot," *2023 IEEE International Conference on Robotics and Automation (ICRA)*, IEEE, 2023, pp. 11396–11403.

[13] Trotta, A., Felice, M. D., Montori, F., Chowdhury, K. R., and Bononi, L., "Joint Coverage, Connectivity, and Charging Strategies for Distributed UAV Networks," *IEEE Transactions on Robotics*, Vol. 34, No. 4, 2018, pp. 883–900. https://doi.org/10.1109/TRO.2018.2839087.

[14] Qin, W., Shi, Z., Li, W., Li, K., Zhang, T., and Wang, R., "Multiobjective routing optimization of mobile charging vehicles for UAV power supply guarantees," *Computers & Industrial Engineering*, Vol. 162, 2021, p. 107714. https://doi.org/https://doi.org/10.1016/j.cie.2021.107714, URL https://www.sciencedirect.com/science/article/pii/S0360835221006185.

[15] Moore, B., Carlson, S. J., Arora, P., Avlonitis, E. S., Karakurt, T., Feil-Seifer, D., and Papachristos, C., "Combined Docking-and-Recharging for a Flexible Aerial/Legged Marsupial Autonomous System," *2023 IEEE Aerospace Conference*, IEEE, 2023, pp. 1–9.

[16] Arora, P., Karakurt, T., Avlonitis, E., Carlson, S. J., Moore, B., Feil-Seifer, D., and Papachristos, C., "Deep Learning–based Reassembling of an Aerial & Legged Marsupial Robotic System–of–Systems," *2023 International Conference on Unmanned Aircraft Systems (ICUAS)*, IEEE, 2023, pp. 626–633.

[17] Seyedi, S., YazicioÄŸlu, Y., and Aksaray, D., "Persistent Surveillance With Energy-Constrained UAVs and Mobile Charging Stations," *IFAC-PapersOnLine*, Vol. 52, No. 20, 2019, pp. 193–198. https://doi.org/https://doi.org/10.1016/j.ifacol.2019.12.157, URL https://www.sciencedirect.com/science/article/pii/S2405896319320087, 8th IFAC Workshop on Distributed Estimation and Control in Networked Systems NECSYS 2019.

[18] Ko, Y. K., Park, J. H., and Ko, Y. D., "A Development of Optimal Algorithm for Integrated Operation of UGVs and UAVs for Goods Delivery at Tourist Destinations," *Applied Sciences*, Vol. 12, No. 20, 2022. https://doi.org/10.3390/app122010396, URL https://www.mdpi.com/2076-3417/12/20/10396.

[19] Rovira-Sugranes, A., Razi, A., Afghah, F., and Chakareski, J., "A review of AI-enabled routing protocols for UAV networks: Trends, challenges, and future outlook," *Ad Hoc Networks*, Vol. 130, 2022, p. 102790. https://doi.org/https://doi.org/10.1016/j.adhoc.2022.102790, URL https://www.sciencedirect.com/science/article/pii/S1570870522000087.

[20] Zhang, Q., Jiang, M., Feng, Z., Li, W., Zhang, W., and Pan, M., "IoT Enabled UAV: Network Architecture and Routing Algorithm," *IEEE Internet of Things Journal*, Vol. 6, No. 2, 2019, pp. 3727–3742. https://doi.org/10.1109/JIOT.2018.2890428.

[21] Wang, Z., Yao, H., Mai, T., Xiong, Z., and Yu, F. R., "Cooperative Reinforcement Learning Aided Dynamic Routing in UAV Swarm Networks," *ICC 2022 - IEEE International Conference on Communications*, 2022, pp. 1–6. https://doi.org/10.1109/ICC45855.2022.9838808.

[22] Zhai, W., Liu, L., Peng, J., Ding, Y., and Lu, W., "PAR: A Power-Aware Routing Algorithm forÂ UAV Networks," *Wireless Algorithms, Systems, and Applications*, edited by L. Wang, M. Segal, J. Chen, and T. Qiu, Springer Nature Switzerland, Cham, 2022, pp. 333–344.

[23] Zhang, Z., Liu, X., and Feng, B., "Research on obstacle avoidance path planning of UAV in complex environments based on improved Bézier curve," *Scientific Reports*, Vol. 13, No. 1, 2023. https://doi.org/10.1038/s41598-023-43783-7, URL http://dx.doi.org/10.1038/s41598-023-43783-7.

[24] Li, H., Zhu, J., Liu, Y., and Fu, X., "Autonomous Obstacle Avoidance Algorithm for UAVs Based on Obstacle Contour Detection," *Advances in Guidance, Navigation and Control*, edited by L. Yan, H. Duan, and Y. Deng, Springer Nature Singapore, Singapore, 2023, pp. 584–593.

[25] Huda, S. A., and Moh, S., "Survey on computation offloading in UAV-Enabled mobile edge computing," *Journal of Network and Computer Applications*, Vol. 201, 2022, p. 103341. https://doi.org/https://doi.org/10.1016/j.jnca.2022.103341, URL https://www.sciencedirect.com/science/article/pii/S1084804522000108.

[26] Song, Z., Qin, X., Hao, Y., Hou, T., Wang, J., and Sun, X., "A comprehensive survey on aerial mobile edge computing: Challenges, state-of-the-art, and future directions," *Computer Communications*, Vol. 191, 2022, pp. 233–256. https://doi.org/https://doi.org/10.1016/j.comcom.2022.05.004, URL https://www.sciencedirect.com/science/article/pii/S0140366422001566.

[27] Srivastava, A., and Salapaka, S. M., "Simultaneous facility location and path optimization in static and dynamic networks," *IEEE Transactions on Control of Network Systems*, Vol. 7, No. 4, 2020, pp. 1700–1711.

[28] Tranzatto, M., Mascarich, F., Bernreiter, L., Godinho, C., Camurri, M., Khattak, S. M. K., Dang, T., Reijgwart, V., Loeje, J., Wisth, D., Zimmermann, S., Nguyen, H., Fehr, M., Solanka, L., Buchanan, R., Bjelonic, M., Khedekar, N., Valceschini, M., Jenelten, F., Dharmadhikari, M., Homberger, T., De Petris, P., Wellhausen, L., Kulkarni, M., Miki, T., Hirsch, S., Montenegro, M., Papachristos, C., Tresoldi, F., Carius, J., Valsecchi, G., Lee, J., Meyer, K., Wu, X., Nieto, J., Smith, A., Hutter, M., Siegwart, R., Mueller, M., Fallon, M., and Alexis, K., "CERBERUS: Autonomous Legged and Aerial Robotic Exploration in the Tunnel and Urban Circuits of the DARPA Subterranean Challenge," *Field Robotics*, 2021, pp. 274–324, arXiv.2201.07067.